High-Speed and High-Power GaSb Based Photodiode for 2.5 μm Wavelength Operations

Rui-Lin Chao[1,2], Jhih-Min Wun[1], Yu-Wen Wang[1], Yi-Han Chen[1], J. E. Bowers[3], and Jin-Wei Shi[2,3*]
[1]*Department of Photonics, National Chiao-Tung University, Hsinchu 300, Taiwan*
[2]*Department of Electrical Engineering, National Central University, Taoyuan 320, Tawian*
**Tel: +886-3-4227151 ext. 34466, *FAX: +886-3-4255830*
**Email: jwshi@ee.ncu.edu.tw*
[3]*Department of Electrical and Computer Engineering, University of California Santa Barbara, CA, 93106.*

Abstract: By using partially depleted $Ga_{0.8}In_{0.2}As_{0.16}Sb_{0.84}$ absorber in GaSb based photodiodes for 2.5 μm wavelength operation, such device achieves high-speed and high-saturation current (3.6 mA/6 GHz) performances with low dark current (0.7μA at -2V). Device modeling results suggest that the internal carrier response time limits its dynamic performance.

I. Introduction

2 μm high-speed photodiodes play vital role in the applications of mid-infrared (2-5 μm) Si photonics [1], high-resolution active light detection and ranging (LIDAR) sensors [2], and photo-receivers in new generation optical fiber communication systems [3,4]. In this paper, we demonstrate a novel GaSb based p-i-n photodiode, which has a cut-off wavelength at ~2.5 μm and a partially depleted p-type $Ga_{0.8}In_{0.2}As_{0.16}Sb_{0.84}$ absorption layer in order to simultaneously achieve high-speed and high-power performance [5]. As compared to the reported InP based PDs [2,4] with a cut-off wavelength at around 2 μm, our proposed device structure here is lattice-matched grown on a n-type GaSb substrate and the thick fully-relaxed $InAs_xP_{1-x}$ [2] or $In_xGa_{1-x}As$ [4] buffer layers grown on InP substrate can be totally eliminated. Furthermore, the GaSb based PD with a thick lattice-matched $Ga_xIn_{1-x}As_ySb_{1-y}$ alloy as photo-absorption layer can further extend its detection wavelength window to as long as ~4 μm [6], which covers most of the mid-infrared wavelengths (2-5 μm). The modeling and measurement results suggest that the slow carrier drift/diffusion time in our $Ga_{0.8}In_{0.2}As_{0.16}Sb_{0.84}$ active layers are major limiting factors in its speed and output power.

II. Device Structure

Figure 1 (a) is a photo of the top-view of the fabricated device. Here, we adopted the structure of a typical vertical-illuminated photodiode with an active circular mesa and a p-type contact on the top. The diameter of the mesa is 8 or 10 μm. The whole epi-layer structure is grown on a 3-inch n-type GaSb substrate. From top to bottom, it is composed of a 10 nm p^+ GaSb (Be doped: 1×10^{19} cm^{-3}) ohmic contact layer, a 10 nm $Al_{0.5}Ga_{0.5}Sb$ p^+ (1×10^{19} cm^{-3}) diffusion blocking layer, a 1.1 μm $Ga_{0.8}In_{0.2}As_{0.16}Sb_{0.84}$ photo-absorption layer, and a 700 nm N-type (Te doped: 8×10^{17} cm^{-3}) GaSb contact layer. The photoluminescence (PL) measurement result of our device structure is given in Figure 1 (b) showing the PL peak at 2.5 μm wavelength, which represents the absorption-edge wavelength of our proposed PD structure. In our thick (1.1 μm) $Ga_{0.8}In_{0.2}As_{0.16}Sb_{0.84}$ photo-absorption layer, there is a 400 nm p-type un-depleted layer with a graded doping profile (5×10^{19} cm^{-3} (top) to 5×10^{17} cm^{-3} (bottom)) to further enhance its saturation output power performance. The fabricated device is carefully passivated by the SiO_2 film grown near room temperature to avoid surface damage induced leakage current. As shown in Figure 1 (a), for the purpose of on-wafer measurement, the fabricated device is integrated with a co-planar waveguide (CPW) pad on the GaSb substrate with deposited SiO_2 film on top of it to avoid the leakage current from n-type GaSb substrate.

III. Measurement Results

Figure 2 (a) and (b) shows three typical current (I)-voltage (V) curves of fabricated devices with 8 and 10 μm active diameters, respectively. As can be seen, both devices can have significant rectifying behavior with a low dark current under high reverse bias voltage. Under forward bias operation with a turn-on voltage at ~0.5V, the measured differential resistance for both devices is nearly the same as ~140 Ω, which is mainly originated from the contact and bulk resistance of n-type GaSb layers. Thanks to our device passivation process, the measured dark current of both devices with a miniaturized active diameter 8 (10) μm is as small as 0.7-1 (1~2.8) μA under -2V bias, which is the typical operation bias voltage for high-speed performance of our device under low output photocurrent operation. The reported dark current values here are close with that of state-of-the-art InP based 2 μm wavelength PDs (several μAs) [3] with a close optical-to-electrical (O-E) bandwidth performance, which will be discussed latter. Under 1.55 μm wavelength excitation and -2 V bias, the measured DC responsivity is around 0.4 A/W, which corresponds to 32% external quantum efficiency. This result indicates a much higher defect density and smaller mobility of photo-generated carrier in our p-type $Ga_{0.8}In_{0.2}As_{0.16}Sb_{0.84}$ absorber than that of InP based $In_{0.53}Ga_{0.47}As$ p-type absorber [7]. Figure 3 (a) and (b) shows the measured power dependent optical-to-electrical (O-E) frequency responses under a fixed reverse bias voltage (-4V) of devices with 8 and 10 μm active diameter, respectively. Such measurement is realized by use of a light-wave component analyzer at 1.55 μm wavelength. The dotted line in such Figure represents the extracted RC-limited frequency response of each device by use of the equivalent-circuit modeling technique [7]. As can be seen, under a small output photocurrent (0.05 mA), the widest 3-dB O-E bandwidth is around 6 and 3.6 GHz, for 8 and 10 μm active diameter, respectively. By use of these measured net O-E and extracted RC-limited bandwidths, we can further extract the internal transit time limited bandwidth (f_T) of our device. As shown in Figure 4, the

978-1-5090-1906-9/16/$31.00

intercept in the axis of $1/f_{3dB}$ represents that the extracted f_T is around 7.6 GHz. According to extracted f_T and our calculation based on drift-diffusion model [7], the corresponding drift-velocity and mobility of electron and hole in the $Ga_{0.8}In_{0.2}As_{0.16}Sb_{0.84}$ absorption layer are all much smaller than those in $In_{0.53}Ga_{0.47}As$ absorption region. The slow drift carrier induced space-charge screening effect thus becomes the major limiting factor of saturation current. Figure 5 (a) and (b) represents the bias dependent (-3, -4, and -6 V) photo-generated radio-frequency (RF) power measured at 6 and 3 GHz of devices with 8 and 10 μm active diameter, respectively. The ideal relation between the RF power of a 100% modulated large-signal and the average current for a 50 Ω load is also plotted for reference. Under -6 V bias, the highest saturation current is around 3.5 and 4 mA for devices with 8 and 10 μm active diameter, respectively.

IV.Summary

A high-speed and high-power GaSb based PD with cut-off wavelength at around 2.5 μm was demonstrated for the first time. The partially depleted absorber has been implemented in our structure to minimize the space-charge screening effect and improve its high-power/speed performance. Internal transit time limited O-E bandwidth at 6 GHz and 3.6 mA saturation current with low dark current performance has been successfully demonstrated.

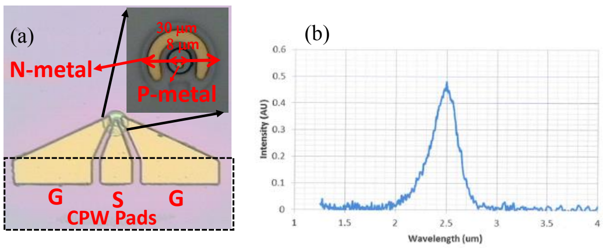

Figure 1. (a) Top-view of demonstrated device. G: ground. S: signal. (b) Measured PL spectrum of epitaxy wafer used for device fabrication.

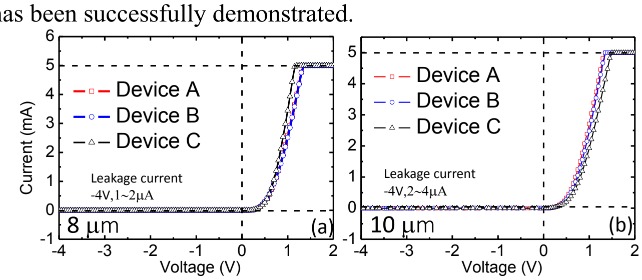

Figure 2. The measured dark I-V curves of devices with (a) 8 μm (b) 10 μm active diameters.

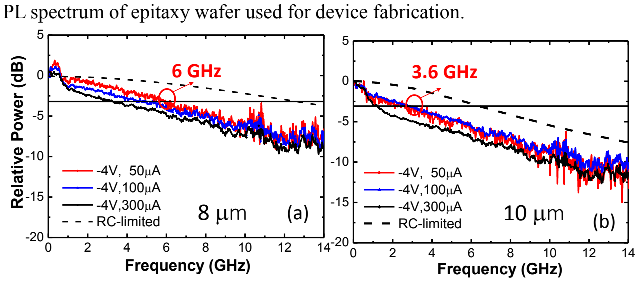

Figure 3. The measured O-E frequency responses of devices with (a) 8 μm and (b) 10 μm active diameters under different output photocurrents and a fixed reverse bias voltage at -4 V.

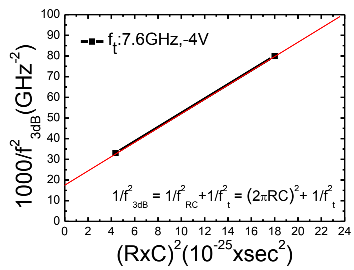

Figure 4.Extrcated RC-time constant ($1/f_{RC}$) versus net O-E bandwidths ($1/f_{3dB}$) of devices with 8 and 10 μm active diameters

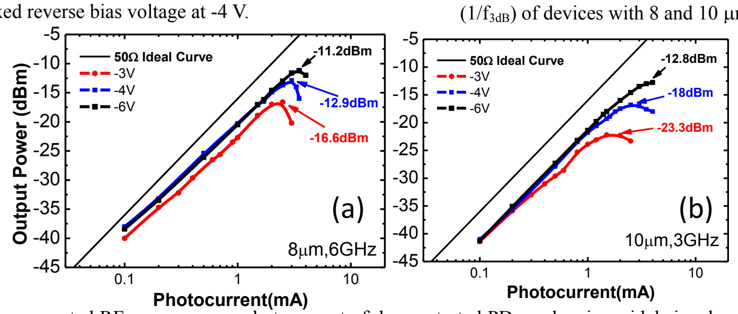

Figure 5. Measured photo-generated RF power versus photocurrent of demonstrated PDs under sinusoidal signal excitations and different reverse biases at an operating frequency of (a) 6 GHz (8 μm device) and (b) 3 GHz (10 μm device). The solid line shows the ideal trace for a 100% modulation depth and 50 Ω load.

V. Reference:

[1] R. Soref, "Mid-infrared photonics in silicon and germanium," *Nature Photonics,* vol. 4, pp. 495-497, Aug., 2010.

[2] A. Joshi and S. Datta, "High-Speed, Large-Area, p-i-n InGaAs Photodiode Linear Array at 2-micron Wavelength," " *Proc. SPIE, Infrared Technology and Applications XXXVIII,* vol. 8353, pp. 83533D, May, 2012.

[3] J. E. Bowers, A.K. Srivastava, C. A. Burrus, J. C. DeWinter, M. A. Pollack and J. L. Zyskind, "High Speed GaInAsSb/ GaSb PIN Photodetectors for Wavelengths to 2.3 μm," *Electronic Letters,* vol. 22, pp. 137-138, Jan., 1986.

[4] N. Ye, H. Yang, M. Gleeson, N. Pavarelli, H. Zhang, J. O'Callaghan, W. Han, N. Nudds, S. Collins, A. Gocalinska, E. Pelucchi, P. O'Brien, F. C. G. Gunning, F. H. Peters, and B. Corbett, "InGaAs Surface Normal Photodiode for 2 μm Optical Communication Systems," *IEEE Photon. Technol. Lett.,* vol. 27, pp. 1469-1472, July, 2015.

[5] X. Li, N. Li, X. Zheng, S. Demiguel, J. C. Campbell, D. A. Tulchinsky, and K. J. Williams, "High-Saturation-Current InP-InGaAs Photodiode With Partially Depleted Absorber," *IEEE Photon. Technol. Lett.,* vol. 15, pp. 1276-1278, Sep., 2003.

[6] A. Rakovska, V. Berger, X. Marcadet, B. Vinter, G. Glastre, T. Oksenhendler, and D. Kaplan, "Room temperature InAsSb photovoltaic midinfrared detector," *Appl. Phys. Lett.*, vol. 77, no. 3, pp. 397-399, July, 2000.

[7] Jin-Wei Shi, Kai-Lun Chi, Chi-Yu Li, and Jhih-Min Wun "Dynamic Analysis of High-Efficiency InP Based Photodiode for 40 Gbit/sec Optical Interconnect across a Wide Optical Window (0.85 to 1.55 μm)," *IEEE/OSA Journal of Lightwave Technology,* vol. 33, no. 4, pp. 921-927, Feb., 2015.